



## Performance of Concatenated 2D MAP for Multi-track Signal Detection

M. D. Almustapha\*, M. T. Kabir, H. A. Abdulkareem, N. B. Gafai#

Department of Telecommunications Engineering, Ahmadu Bello University, Zaria – Nigeria.

#Department of Electrical Engineering, Baze University, Abuja – Nigeria.

\*[md.almustapha@gmail.com](mailto:md.almustapha@gmail.com)

Research Article

### Abstract

A low complexity two-dimensional (2D) detection technique for multi-track two-dimensional magnetic recording (TDMR) channel with shingled magnetic recording (SMR) media was presented in this paper. The technique involves the use of serially concatenated 2D maximum a posteriori (MAP) and a regular MAP detector for multi-track joint detection of a 2D signal. 2D MAP detector was applied in the along-track direction to cancel the inter-symbol interference (ISI), while the regular MAP detector was used across-tracks for inter-track interference (ITI) cancellation. The results show that the serially concatenated 2D MAP with regular MAP detector has less detection complexity as compared to full 2D detector when implemented for joint signal detection on an 8-track SMR media.

Copyright © Faculty of Engineering, Ahmadu Bello University, Zaria, Nigeria.

### Keywords

Two-dimensional magnetic recording; Bahl Cocke Jelinek Raviv detector; Maximum a-posteriori decoding; Shingled magnetic recording; Inter-symbol interference; inter-track interference.

### Article History

Received:– March, 2022

Accepted:– April, 2022

Reviewed:– March, 2022

Published:– April, 2022

### 1. Introduction

Two-dimensional magnetic recording (TDMR) is a promising technology for future magnetic recording systems. It is among the candidate technologies proposed for increasing the areal density of magnetic recording systems. TDMR uses a combination of the Shingled magnetic recording (SMR) and 2D readback equalisation and detection techniques to increase the areal density capacity beyond the convention limit of the magnetic recording system (Wood *et al.*, 2009). Unlike in the conventional magnetic recording system where interference is only along the down track direction (that is ISI only); in TDMR system, the interferences are present in both along track (ISI) and across tracks (ITI) directions culminating into a 2D interference problem (Chan *et al.*, 2010). Therefore, for the signal to be fully recovered in the TDMR system, both the ISI and ITI contributions to the signal must be considered in the equalisation and detection processes. This however results in an increase complexity of the 2D detector which is in exponential order to the number of tracks and data bits involved (Srinivasa *et al.*, 2014).

In a multi-track TDMR system, joint-track detection is carried out by either applying a linear equaliser to cancel the interference in one direction and partial response maximum likelihood (PRML) detection in the other direction (Srinivasa *et al.*, 2014), or full 2D SOVA (Abdulrazaq *et al.*, 2015), (Zheng *et al.*, 2014). While using a linear equaliser reduces the detection complexity, there is a loss of performance incurred at extreme ISI and ITI conditions. The full 2D SOVA provides better detection performance but have higher complexity compared to the former. The complexity of the full 2D detectors for joint-track detection is in an exponential order of  $2^{wk}$  where,  $w$  represents the number of tracks and  $k$  represents number of

bits involved. This limits their deployment especially when more tracks are involved. Besides the computational complexity, most 2D detectors especially ML detectors applied in along track direction do not fully utilize the information available from the other direction, since the detector is applied only along one of the directions. This degrades the detection performance when the interference from the other direction is high. An optimum detection strategy is therefore needed.

An optimal 2D detector carries out multi-track joint 2D detection across all tracks to fully exploit the 2D interferences present in both directions (Abdulrazaq *et al.*, 2015). Although it suffers from high implementation cost, its implementation seems increasingly feasible in future recording systems with the current improvement in CMOS technology deployment (Kim, 2012). A multi-track 2D SOVA for joint track detection of SMR media was proposed in (Zheng *et al.*, 2017). The 2D SOVA detects data jointly from multiple tracks in the presence of 2D interference. In (Zheng *et al.*, 2014) a low-complexity 2D SOVA designed to reduce the complexity of the multi-track 2D SOVA was presented. However, in both detectors, 2D SOVA is applied in the down track direction only, since multiple tracks were considered jointly. This results in performance degradation when the ITI across tracks is high. Meanwhile, a 2D SOVA concatenated with a regular Viterbi detector was proposed for detection of data from SMR media in (Muhammad *et al.*, 2015). Although the detection complexity was reduced, the 2D SOVA and the Viterbi detectors employed do not fully exploit the trellis structure completely in determining the reliability of the decoded bits. A better result and performance can be achieved with optimal 2D MAP and regular MAP detector that exploit the trellis structure by incorporating all the

branch metric probabilities in its computations. This ensures that no valuable information on a bit position a priori or a posteriori is discarded, unlike the former case, where a select few information bits after the given bit position are utilized and the rest are discarded.

In this paper, we present a serial concatenation of 2D MAP with a regular MAP Detector for multitrack detection of two-dimensional signal of a shingled magnetic media. The 2D MAP detector is applied along track to cancel the effect of ISI in the down track direction while a regular MAP detector across tracks is used to remove the effect of ITI. This used to perform multi-track joint detection of multiple tracks in order to extract information from a TDMR system using the SMR media.

The rest of the paper is organised as follows. Section II gives an overview of the channel model, shaping equaliser and 2D MAP detection; section III elaborates on the modelling and design of the detectors; section IV evaluates the features of the two detectors used in getting the results; section V presents some results from the designs and their comparisons, and section VI presents conclusions drawn from the results.

## 2. Overview of Channel and Equalization

### 2.1 SMR Channel

The SMR channel can be implemented using the conventional perpendicular magnetic recording media (PMR) without the need for redesigning the media structure. This makes it very attractive for deployment compared to order candidate technologies; bit pattern magnetic recording (BPMR), heat assisted magnetic recording (HAMR) which require new media (Shiroishi *et al.*, 2009). Therefore, in this paper the SMR channel used is modelled based on the existing PMR channel model.

In the PMR media, data bits are read from the media by a magneto-resistive (MR) read-head in the form of magnetisation bits which are stored on the magnetic disc. The read-head picks the magnetisation of a point on disk a distance away before reaching or after passing the bit position. This results in inter-Symbol interference (ISI) of neighbouring bits. The isolated channel response of the PMR media as read by the MR read-head representing the magnitude of the magnetic field is modelled as (Wu *et al.*, 2009);

$$S(t) = V_{\max} \tanh\left(\frac{2t}{0.579\pi T_{50}}\right) \quad (1)$$

where  $V_{\max}$  is the peak signal amplitude,  $t$  is the sampling time and  $T_{50}$  is the time taken for the response to change from  $-V_{\max}/2$  to  $+V_{\max}/2$ .

The readback signal from the channel can be represented as the superposition of isolated transition response expressed as (Wu *et al.*, 2009);

$$Z(t) = \sum_i d_i s(t + a_i - iB) \quad (2)$$

Where  $B$  is the channel bit period,  $a_i$  is a random Gaussian variable representing the jitter noise due transition jitter, and  $d_i$  represents the data transitions computed as;

$$d_i = \frac{x_i - x_{i-1}}{2}, \quad x_i \in \{-1, +1\} \quad (3)$$

The dipulse response for the channel is given by;

$$h(t - iB) = \frac{s(t - iB) - s(t - i(B + 1))}{2} \quad (4)$$

Substituting  $d_i$  with (3), taking the Taylor's expansion of (2) and truncating the higher order approximations gives,

$$Z(t) = \sum_i x_i h(t - iB) + \sum_i d_i a_i s'(t - iB) \quad (5)$$

The first term in (5) is the convolution of the data with the channel response representing the data transition whereas the second term represents the first order approximation of the jitter noise.

In SMR media, due to the shingled writing of closely overlapped tracks, there is ITI from the side tracks in the process of reading data from the main track. This need to be included into the readback signal. Therefore, the data ( $y$ ) of track  $N$  will contributions from signal components of the track preceding and succeeding it.

That is for any bit position " $i$ ",

$$y_j(i) = \sum_{j=N-n_1}^{N+n_2} w_j Z_j(i) \quad (6)$$

Where  $w_j$  is the fraction of the adjacent channels contributed to the signal  $y_j(i)$ ,  $n_1$  and  $n_2$  are the number of tracks preceding and succeeding the read track respectively.

Therefore, the total signal is the sum of all interfering signals contribution within a given track and other neighbouring tracks including other noises modelled as additive white Gaussian ( $n_{i,j}$ ) is expressed in equation (7).

$$y_{i,j} = \sum_j \sum_i x_{i,j} h_{i,j} + \sum_j \sum_i d_{i,j} a_{i,j} s'_{i,j} + n_{i,j} \quad (7)$$

The variables " $hi$ " and " $s'ir$ " are used in place of  $h(t-iB)$  and  $s'(t-iB)$  for easier writing.

### 2.2 Equalization

After reading the signal from the 2D channel, the data is shaped to the desired 2D target before detection in order to reduce the complexity of the detector and also to improve system performance (Shah *et al.*, 2007). In the 2D system, because of the interferences from both sides (along track ISI and across tracks ITI), two equalisers are used in turns for both directions in order to shape the data into the desired 2D target response. The equaliser applied along the track is a PR equaliser in which the coefficients needed to shape the data to the required target are derived by evaluating the matrix equation as expressed in equation (8).

$$E = H^{-1}T \quad (8)$$

Where  $E$  gives the equaliser coefficients required to transform the signal shape to that of the desired target response, while  $H$  is the matrix approximation of the channel

response.  $T$  is a column matrix formed by a target vector of equaliser size padded with zeros on both sides.

### 2.3 MAP Detection

The maximum a posteriori (MAP) detector is a detector designed to determine the most probable bits or symbols that are received. Unlike a maximum likelihood sequence detector (MLSD) which minimizes the probability of sequence error. MAP detection is implemented in this paper using the Bahl Cocke Jelinek Raviv (BCJR) algorithm. The BCJR algorithm utilizes the trellis structure with the a priori probability in determining the a posteriori probability of the decoded bits (Bahl *et al.*, 1974) (1 or 0) using Equation (9).

$$APP(x_i) = \sum_{s_{k-1}^n, s_k^n} \alpha_{k-1}(s_{k-1}^n) \cdot \beta_k(s_k^n) \cdot \gamma_k^{x_{k=i}}(s_{k-1}^n, s_k^n) \quad (9)$$

The expression in (9) gives the sum of the joint probability in transiting from the previous state to the current state after receiving the data bit  $x_i$ . The first and second terms of the equation are the forward and backward state probabilities, while the third term denotes the trellis branch transition probability. The forward and backward state probabilities are computed recursively using the Equations (10) and (11) respectively (Bahl *et al.*, 1974).

$$\alpha_k(s_k^n) = \sum_{s_{k-1}^n} \alpha_{k-1}(s_{k-1}^n) \cdot \gamma_k^{x_{k=i}}(s_{k-1}^n, s_k^n) \quad (10)$$

$$\beta_k(s_k^n) = \sum_{s_{k+1}^n} \beta_{k+1}(s_{k+1}^n) \cdot \gamma_k^{x_{k=i}}(s_{k+1}^n, s_k^n) \quad (11)$$

For this paper, the trellis path transition probabilities or the branch probabilities are given by,

$$\gamma_k^{x_{k=i}}(s_{k-1}^n, s_k^n) = \exp\left(-\frac{x_k - y_n}{2\sigma^2}\right) \quad (12)$$

where  $x_k$  is the received symbol or bit at time  $t$ ,  $y_n$  is the ideal symbol or bit at time  $t$ .  $\sigma^2$  is the channel noise variance

## 3. 2D Multi-Track Map Detector

### 3.1 2D (Multi-level) Multi-track MAP Detector for ISI Cancellation along Track.

In a single track/binary level MAP detector with target length 3, there are four states in the trellis with two incoming and outgoing branches per state. However, for multilevel MAP detector where more than one bit is received, the number of transitions per branch is  $2^k$  and the number of states is  $2^{m \times k}$ , where “ $m$ ” is the constraint length ( $Target - 1$ ) of the detector, and “ $k$ ” represents the number of bits (interfering tracks) involved. For instance, if two tracks are considered (ITI of two tracks), there are 4 branches per state and 16 of states in the trellis for a target length 3. Similarly, when ITI from three tracks is considered, there will be 8 branches per state and 64 states (for target length 3) in the trellis.

In our implementation, we consider ITI from two tracks and a target length 4. Therefore, a trellis with 64 states and 4 branches transiting from each state was used for the detector along track direction for ISI cancellation. Fig. 1 shows the trellis diagram for the 2D MAP detector along track. To implement the detector, the branch transition probability ( $\gamma$ ) for each branch is determined using (12) across the whole trellis. The values of  $\gamma$  are normalised by dividing each and every value of  $\gamma$  by the total of the  $\gamma$ 's. The normalised  $\gamma$  for each branch now corresponds to the dibit response for that branch. After all the  $\gamma$ 's are determined, the next stage is to initialise the forward recursive probability ( $\alpha$ ) for all states, for the first received symbols.

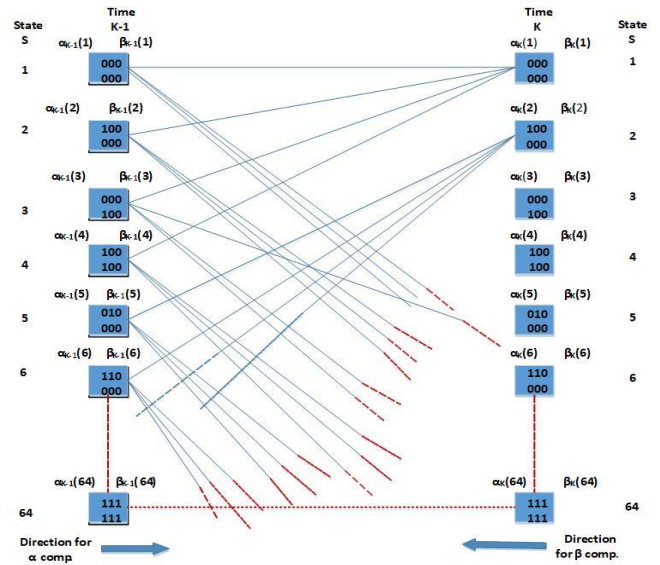


Figure 1: Trellis diagram for the 2D MAP detector along-track with target length 4 and two-track ITI.

In determining  $\alpha$ , for the first state is given a value of 1, while 0 is assigned to the  $\alpha$ 's for other states. The  $\alpha$ 's for the next state transition is determined by multiplying  $\gamma$  with the  $\alpha$  of the state from which the branch originates to get the branch transition probability using (10). The branch transition probabilities that terminate at the same state are then summed up to give the  $\alpha$  of the new state for the next symbols. The  $\alpha$  values determined at each instance are normalised to prevent having all zero values. All the  $\alpha$ 's determined for each time instance are saved up to the last data of the track.

When all the  $\alpha$ 's are determined and saved, the backward recursion then begins by initialising the backward recursive probability ( $\beta$ ) for all states, for the last received symbols at the end of the trellis. The first state is given  $\beta$  of 1, while the rest are assigned  $\beta$  of 0. The  $\beta$ 's for all states at each time interval are determined using the same procedure used in determining  $\alpha$ 's except it is started backward from the end to the beginning of the trellis (using (11)). After all the  $\gamma$ ,  $\alpha$ ,  $\beta$ , are determined across the whole trellis, the APP of each pair of the received symbols being [0, 0], [0, 1], [1, 0], and [1, 1] is determined using (9). The  $\alpha$  for each state is multiplied by

the  $\gamma$  of the branches originating from that state, and then multiplied to the  $\beta$  of the state to which the branches transitioned to. This produces the branch APPs probabilities for each branch transition. The APPs are then normalised to prevent the occurrence of all zero values.

When all the tracks are processed, the APPs are stored in history register to be used as the branch metrics for the MAP detector across tracks for ITI cancellation.

### 3.2 Across-Track MAP Detector ITI Cancellation

Once all the tracks are processed, the saved APPs from the output of the multi-level 2D MAP detector along the track are now used as the branch metrics for detector used across tracks for the ITI cancellation. The first bits of all the tracks are now considered in a sequential manner. That is to say, the first bit on track one is considered as the first data bit, then followed by the first bit on track two as the second data bit, and so on until all the data bits on the tracks are processed. The MAP detector across tracks has a reduced trellis structure with two states and two branches per state as shown in Figure 2. The saved APPs representing the four possible probabilities now serve as the total number of branch metrics. The  $\alpha$ 's and  $\beta$ 's are determined using the initial conditions, and the saved APPs from the 2D MAP detector along track as the new branch metrics ( $\gamma$ ).

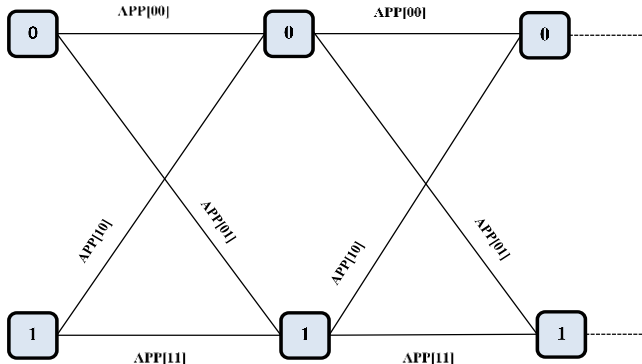


Figure 2: Reduced Trellis diagram of MAP detector across-track

After all the  $\alpha$ 's and  $\beta$ 's determined, the APP of each symbol being either a 1 or a 0 is determined across the tracks. This process is continued until all the data from all the tracks are detected sequentially. This again produces the branch APPs for the ITI detector across tracks. The APP of 0 is obtained by adding up the branch APPs whose transition is produced due to the bit 0, and the APP of 1 is produced by adding up those due to the bit 1. The final output data across tracks is decided based on the highest APP value. This detects the data out of ITI.

## 4. Simulation and Design Evaluation

### 4.1 Simulation Model

The simulation model was developed and implemented using C/C++ programming environment. Data to be recorded on the disk was assumed to be written on a sector of 8 tracks with 4096 bits each. A guard band containing -1's (0s) all through is placed between sector separations during the write

process. The SMR channel was considered to have ITI of two tracks. A portion of the first track was assumed to contain -1s written all through and the last track of a sector is assumed to be two times larger than the others. This ensures that succeeding tracks do not overwrite the extra width of the last track.

Jitter noise power was set to constitute 80% of the total signal noise power while AWGN constitutes the remaining 20% of the total signal noise power. The overall signal SNR in dB is calculated as,

$$SNR = 10 \log \left( \frac{V_p^2}{\sigma_j^2 + \sigma_w^2} \right) \quad (13)$$

Where  $V_p$  is the peak voltage of the read back signal waveform.  $\sigma_j$  and  $\sigma_w$  are the standard deviations of jitter noise and AWGN respectively.

The initialisation phase begins by evaluating the channel isolated channel response  $h(t)$  and the jitter response ( $s'$ ) using the set values of  $T_{50}$  and  $V_{max}$ . Due to the ITI introduced into the system, the factor for modifying the amplitude of the jitter response in (7) is modified in order to include the ITI response. Thus, the factor modifying the jitter response amplitude for 2D channel application is given (14),

$$J = \sqrt{0.5 \sum (s')^2 \sum (\rho)^2} \quad (14)$$

Where ( $s'$ ) is the jitter response of the channel and  $\rho$  represent the ITI response.

$$\rho = [\alpha_1, \alpha_2] \text{ for two track ITI.}$$

Where  $\alpha_1$  and  $\alpha_2$  represent the fraction of the total amplitude read by the Read head from the two tracks. Figure 5.1 shows the SMR channel model with sector dimension used for this work and how ITI from the side track is read by the Read head. Hence, ITI is incorporated into (14) to account for the signal read by the Read head from the side track.

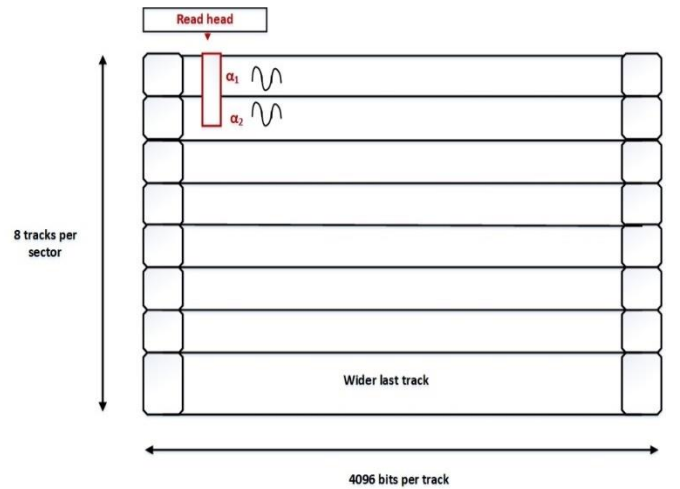


Figure 3: SMR channel model with ITI and sector dimension

For each track, transitions are determined using " $x_{i,j}$ " and saved as " $d_{i,j}$ ". An AWGN with variance  $\sigma_j^2$  is generated, and multiplied, term by term to the transitions  $d_{i,j}$ . The result is then convolved with the jitter response  $s'(t)$  to generate

the jitter noise for each bit position. The saved data  $x_{i,j}$  is also convolved with the channel isolated response  $h(t)$  along the track to generate the ISI data of each track. The resulting ISI data generated is then added to the jitter noise that was already determined above. This gives a signal containing ISI and 1D jitter noise. The signal is then convolved across tracks with the ITI response to produce a 2D interference signal with ISI along the track and ITI across the tracks. The final 2D signal from the channel  $y_{i,j}$  is determined by adding AWGN of variance  $\sigma_w^2$  to the resulting 2D signal above, as demonstrated by (7).

## 4.2 Evaluation

A linear equaliser of length 12 and target [0.4, 1.0, 1.0, 0.4] is employed for shaping the received data along the track. The ITI of the two tracks is used as the target in the across-track direction. The data output from the channel is directly passed into the equaliser along track for shaping and then immediately used for joint track 2D MAP detector to produce 4 metrics (APPs). The resulting 4 metrics are then immediately used for the MAP detector across tracks.

The BCJR algorithm for MAP detection requires separate calculations for  $\alpha$ ,  $\beta$ , and APP determination before an output is produced.  $\alpha$ ,  $\beta$ , and  $\gamma$  values needed to be computed first before the APPs are determined. Therefore, these values need to be saved before APPs are calculated which means a form of memory storage is needed to store  $\alpha$ ,  $\beta$ , and  $\gamma$  with some extra latency incurred in the process. For the 2D MAP, once a data is received after shaping, the  $\gamma$ 's and  $\alpha$ 's for each symbol is determined and saved in memory until the last bit on the track is processed. Then the  $\beta$ 's calculation is started immediately the last bit is received and then immediately used to determine the APPs. This process continues until all the 8 tracks are processed and all the APPs stored in memory as metrics. Therefore, at the end of the 2D detection, a memory capable of storing 4 metrics (APPs) for each of all symbols of a track is required to store the metrics for use by next MAP detector across tracks.

The APPs of the symbols ([0,0], [0,1], [1,0] and [1,1]) represent the metrics of the main track bit of the target along track, with ITI from the succeeding track. In the SMR model, a portion of the first track is assumed to contain -1's written all through. But in actual practice, it is impossible to get -1's written all through due to the random-access nature of the HDDs. It is, however, presented here to ease the detection process. This therefore, reduced the number of possible states of the 2D MAP detector to 8 with 2 branches per state on the first track. This resulted in complexity reduction and provided an improved detection performance. Similar numbers are obtained for the last track in terms of possible states and branches per state since the last track is considered to be wider than the rest. Which means the same data is read on both sides of the main and the interfering track.

For the MAP detector across tracks, when all tracks are processed by the 2D MAP along track, the saved APPs for each state across the trellis section are used as branch metrics for the MAP detector across tracks to cancel ITI. The MAP across tracks starts from one possible state with two branches

originating from it. It then diverges into a 2-state trellis with 2 branches per state and finally terminates into one state at the end of the trellis. The computed APP of the MAP detector across track is taken as the outputted data across the tracks. This data is outputted in groups of 8 bits at a time across tracks and so on until all data bits are outputted.

The latency of a system is an important variable used in evaluating the design of a system. It is the measure of time delay incurred on a system or process between the received of an input to the time when an output is produced. For our own design, the latency incurred is due to the delay produced by the shaping equaliser, delay for metrics determination of the 2D MAP along track and the computational overhead from of MAP detector. The latency is about 2 times the size of a whole sector. This means we have to go first a whole sector size to determine the 4 metrics and go additional sector size before an output is produced across tracks.

## 4.3 Implementation Cost Overhead

The computational operations involved include basic arithmetic operators such as multiplication, addition, subtraction as well as complex arithmetic operations such as exponentiation and comparison operation. In our system implementation, the complexity of the system is analysed in three folds as per producing an output is concerned immediately after a symbol is received. First is the complexity of the shaping equaliser used in transforming the data to the desired form. There is also the complexity of the multi-track 2D MAP detector along track for ISI cancellation, and last is the complexity of the regular MAP detector across tracks for ITI cancellation.

For the shaping equaliser, in shaping the data, all the coefficients of the equaliser are multiplied by the data. This means that the number of multiplication operations performed is equal to the number of the equaliser length employed. The result of the multiplication is then added together to give the output of the shaping equaliser. This implied that the number of additions performed will be one less than the number of multiplications involved. In our implementation, an equaliser of length 12 is used for shaping the data. Therefore, 12 multiplications and 11 additions are needed for shaping the data.

For the multi-track 2D MAP detector, the computational complexity depends on the design of the detector and the target, plus the ITI involved. For target [0.4, 1.0, 1.0, 0.4] and ITI [1, 1] used in this work, the number of possible reference levels obtained is 29 (from -5.6 to 5.6 at steps of 0.4 unit). Therefore, for the branch metric calculations ( $\gamma$  determination) using equation 4.7, 2 multiplications, 1 addition, and 1 exponentiation is required for each reference level to determine the branch metric. This means that a total of 58 multiplications, 29 additions and 29 exponentiations are required for  $\gamma$ 's determination.

To determine  $\alpha$  for the next state,  $\gamma$  is multiplied by the initial  $\alpha$  of the previous state to get the branch probability. The branch probabilities terminating to the next state are then added to produce the  $\alpha$  for that state. In our multi-track 2D MAP detector, there are four incoming and outgoing branches per state. This means that in determining  $\alpha$  for a

state, there are 4 multiplications and 3 additions involved per state. Therefore, a total of 256 ( $4 \times 64$ , for the 64 states) multiplications and 192 ( $3 \times 64$ , for 64 states) additions are need for  $\alpha$ 's determination per symbol processing. Similar numbers (256 multiplications and 192 additions) are also needed for  $\beta$  determination.

The APP is determined by multiplication of  $\alpha$  and  $\gamma$  and then  $\beta$  to get the branch transitional probabilities which are the then added up base on symbols that produced the transition to the various states accordingly. This involves 128 ( $2 \times 64$ ) multiplications and 63 additions for each APP determination. For our two-track ITI model, there are 4 APP levels possible (APP [0, 0], APP [0, 1], APP [1, 0] and APP [1, 1]). This means that in total, there are 512 multiplications and 252 additions involved per symbol processing.

When all tracks are processed, the 4 APP levels from the multi-track 2D MAP detector are saved and used as the metrics for the regular MAP detector across tracks. The detector across tracks has 2 states with 2 incoming and outgoing branches per state. That means 2 multiplications and 1 addition per state is needed for both  $\alpha$  and  $\beta$  determination. This is equivalent to 4 multiplications and 2 additions per symbol processing. The APP of the detector has 2 possible either APP of the symbol received being 0 or 1. Therefore, a total of 8 multiplications and 2 additions are needed per symbol processing for the detector across tracks. Table 1. shows the summary of the complexity per symbol/bit processed (without simplification) of the entire detection scheme proposed for the TDMR channel with two-track ITI and target length 4. In the table, "M" is used as a unit to indicate multiplication operation, "A" represents the addition operation, while "E" is used for exponentiation

Table 1: Computational Complexity

Shaping	12M, 11A
2D BCJR along track	1082M, 665A, 29E
BCJR across tracks	8M, 2A
Total	1102M, 678A, 29E

As comparison with the method presented in (Zheng *et al.*, 2014a) and (Zheng *et al.*, 2014b), where a single full-2D detector is used for joint-track detection, our approach offers significant reduction in the complexity order of the detector. For 8 tracks with a target length of 4, the complexity order of the single full-2D detector is  $2^{8 \times 4} = 4,294,967,296$ . But using the method presented in this work, with ITI of two-tracks and target length of 4, the complexity order of the detector is reduced to  $8 * (2^{2 \times 4}) = 2,048$ .

### 5. Results

The bit error rate (BER) performance of the 2D MAP multi-track detector with target [0.4 1.0 1.0 0.4], ITI [1.0 1.0] (full ITI for both tracks), for varying densities along track (different values of  $T_{50}$ ) is shown in Figure 4. Note that, finding suitable PR target for detection depends on the data density of the channel. Therefore, changing the PR target can affect the performances result of Figure 4 because different PR targets gives different performances for various channel density.

PR target [0.4, 1.0, 1.0, 0.4] which is equivalent to [2.0, 5.0, 5.0, 2.0] was used here because it had the best performance compared to any other target of length 4 at high data density. It is seen that the performance of the detector is best when ISI along track is low ( $T_{50} = 1.0$ ).  $T_{50} = 1.0$  has a gain of about 2dB over  $T_{50} = 1.5$  and almost 6dB compared to  $T_{50} = 2.0$  at BER point  $10^{-3}$ . This is as expected because increasing the data density results in more ISI which generally degrades the performance of the system.

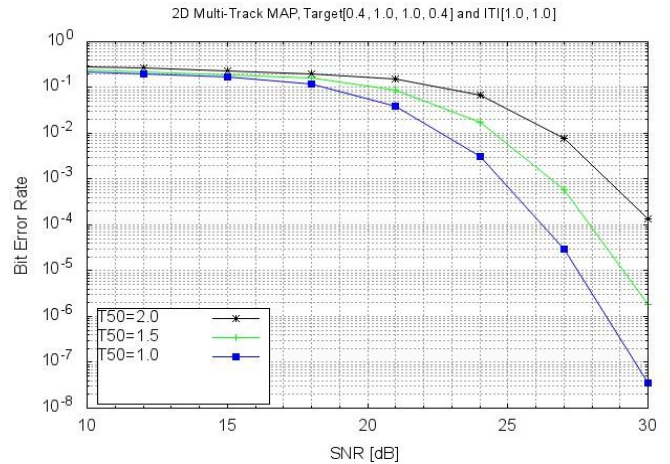


Figure 4: Performance comparison for different data density at ITI [1.0 1.0]

Figures. 5, 6, and 7 show the performance of the multi-track detector at  $T_{50} = 1.0$ ,  $T_{50} = 1.5$ , and  $T_{50} = 2.0$  respectively with varying ITI levels. ITI [1.0 1.0], [1.0 0.75], [1.0 5.0] and [1.0 0.25] gives the contribution of the main track and side track to the overall signal and also, represent the extent to which the side track data interferes with the main track data. In all the three cases ( $T_{50} = 1.0$ ,  $T_{50} = 1.5$ , and  $T_{50} = 2.0$ ), it is observed that different ITI levels have different effect on the performance of the detector. The performance of the detector is best when the ITI is high ([1.0 1.0]) for all ISI condition.

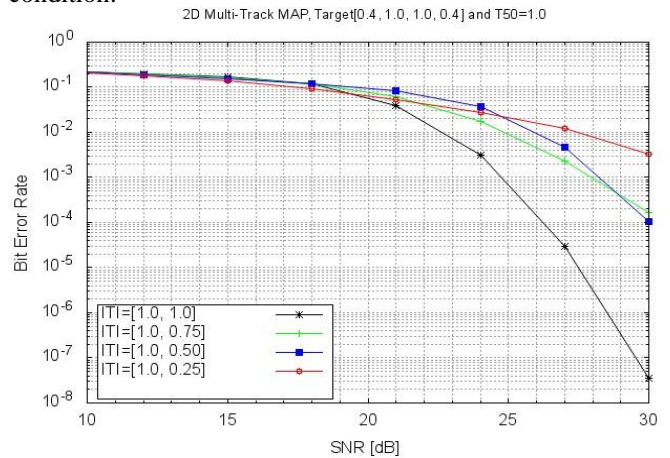


Figure 5: Performance comparison for different ITI levels at  $T_{50} = 1.0$ .

In Figure 5, ITI [1.0 1.0] has a gain of about 4dB over ITI [1.0 0.75] and almost 6dB compared to ITI [1.0 0.25]. The ITIs [1.0 0.75] and [1.0 0.50] show performances that are very close to each other at  $T_{50} = 1.0$ .

Figure 6 shows that the gain recorded for ITI [1.0 1.0] over the other ITIs slightly reduces as the  $T_{50}$  value is increased to  $T_{50} = 1.5$ . The gain reduced to about 4dB for ITI [1.0 1.0] over ITI [1.0 0.75] and 5dB compared to other ITIs. Similar trend is observed in Figure 7 at  $T_{50} = 2.0$ , the gain is reduced to around 3dB and 4dB respectively. The ITI [1.0 1.0] outperformed all the other ITIs due to the fact that, it has the highest minimum separation distance between the different possible symbols of all (see Table 2). This improves the SNR of the captured signal from both tracks by making it higher. Also, the ITI [1.0 1.0] here means that the Read head covers all portion of both tracks capturing more signal energy of the side track, which is beneficial for the 2D detector. However, in practice it is impossible to get all the signal energy of the side track without exceeding into other adjacent tracks. The assumption is made here for analysis purpose.

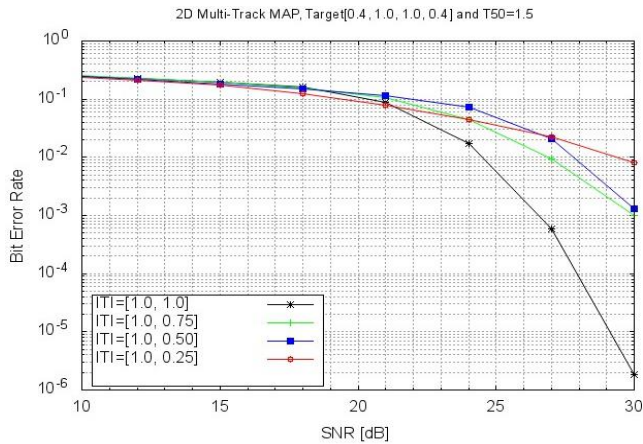


Figure 6: Performance comparison for different ITI levels at  $T_{50} = 1.5$ .

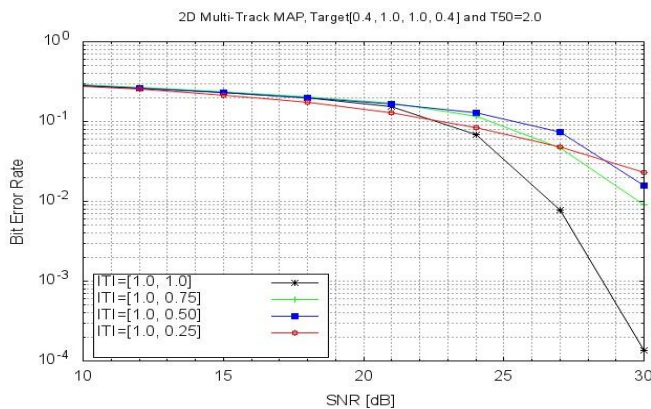


Figure 7: Performance comparison for different ITI levels at  $T_{50} = 2.0$ .

Table 2: Minimum distance separation of ITI targets

ITI	Possible symbol levels	Minimum distance	Ratio to peak level
[1.0 0.25]	1.25, 0.75, -0.75, -1.25	0.5 (1.25 – 0.75)	0.4
[1.0 0.50]	1.50, 0.50, -0.50, -1.50	1 (1.50 – 0.50)	0.66
[1.0 0.75]	1.75, 0.25, -0.25, -1.75	1.5 (1.75 – 0.25)	0.86
[1.0 1.0]	2.0, 0.0, 0.0, -2.0	2 (2.0 – 0.0)	1.0

## 6. Conclusion

A serially concatenated 2D MAP with a regular MAP detector was presented here for multi-track TDMR system using SMR media. It is demonstrated here from the results obtained, that the 2D MAP along track coupled with regular MAP detector across tracks can perform multi-track joint signal detection of a 2D signal with limited complexity as compared to a full 2D detector. This reduces the complexity order from exponential to linear with the number of tracks. Using this approach can improve track density to more than double and also provide good detection performance compared to using the later approach.

## References

Abdulrazaq M. B., Ahmed M. Z., and Davey P. (2015), “Two-dimensional equalization of shingled write disk”, presented in International Conference on Magnetics, ICM2015, (Unpublished).

Bahl, L., Cocke, J., Jelinek, F., & Raviv, J. (1974). Optimal decoding of linear codes for minimizing symbol error rate (corresp.). *IEEE Transactions on information theory*, 20(2), 284-287.

Chan, K. S., Radhakrishnan, R., Eason, K., Elidrissi, M. R., Miles, J. J., Vasic, B., & Krishnan, A. R. (2010). Channel models and detectors for two-dimensional magnetic recording. *IEEE Transactions on Magnetics*, 46(3), 804-811.

Kim K. (2012), “Future silicon technology”. In *Solid-State Device Research Conference (ESSDERC) IEEE, September, 2012 Proceedings of the European* pp. 1-6.

Muhammad, B. A., Mohammed, Z. A., & Paul, D. (2015, November). Concatenated 2D SOVA for two dimensional maximum likelihood detection. In *2015 23rd Telecommunications Forum Telfor (TELFOR)* (pp. 441-444). IEEE.

Shah, P., Ahmed, M. Z., & Kurihara, Y. (2007). New method for generalised PR target design for perpendicular magnetic recording, in *The Eighth Perpendicular Magnetic Recording Conference (PMRC2007)*, Oct 15-17 2007

Shiroishi, Y., Fukuda, K., Tagawa, I., Iwasaki, H., Takenoiri, S., Tanaka, H., ... & Yoshikawa, N. (2009). Future options for HDD storage. *IEEE Transactions on Magnetics*, 45(10), 3816-3822.

Srinivasa, S. G., Chen, Y., & Dahandeh, S. (2014). A communication-theoretic framework for 2-DMR channel modeling: Performance evaluation of coding and signal processing methods. *IEEE transactions on magnetics*, 50(3), 6-12.

Wood, R., Williams, M., Kavcic, A., & Miles, J. (2009). The feasibility of magnetic recording at 10 terabits per square inch on conventional media. *IEEE Transactions on Magnetics*, 45(2), 917-923.

Wu, Z. (2009). *Channel modeling, signal processing and coding for perpendicular magnetic recording*. University of California, San Diego.

Zheng, N., & Zhang, T. (2014). Design of low-complexity 2-D SOVA detector for shingled magnetic recording. *IEEE Transactions on Magnetics*, 51(4), 1-7.

Zheng, N., Venkataraman, K. S., Kavcic, A., & Zhang, T. (2014). A study of multitrack joint 2-D signal detection performance and implementation cost for shingled magnetic recording. *IEEE transactions on magnetics*, 50(6), 1-6.